Desalination and Water Treatment
www.deswater.com

doi: 10.5004/dwt.2020.24967

178 (2020) 322–336
February

Methylene blue removal by nano-polyacrylonitrile particles: modelling and formulation studies

M.S. Mohy Eldin[a,*], S.A. El-Sakka[b], M.M. El-Masry[a], I.I. Abdel-Gawad[b,#], S.S. Garybe[b]

[a]*Polymer Materials Research Department, Advanced Technology and New Materials Research Institute, Scientific Research and Technological Applications City, New Borg El-Arab City 21934, Alexandria, Egypt, emails: mohyeldinmohamed@gmail.com (M.S. Mohy Eldin); mansourelmasry@yahoo.com (M.M. El-Masry)*
[b]*Department of Chemistry, Faculty of Science, Suez University, Alsalam, Suez, Egypt, email: saharelsakka@yahoo.com (S.A. El-Sakka); email: iiabdelgawad@gmail.com (I.I. Abdel-Gawad), smsm_2051@yahoo.com (S.S. Garybe)*

Received 3 January 2019; Accepted 25 September 2019

ABSTRACT

The kinetic and isothermal studies of the methylene blue (MB) adsorption by nano-polyacrylonitrile (PAN) and nano-hydroximated polyacrylonitrile (HPAN) particles prepared by the precipitation polymerization technique have been performed in this study. The kinetic models of the MB adsorption, namely first-pseudo order, second-pseudo order, and Elovich models have been studied over 75 min. The MB concentration was varied between 10 and 50 mg/L during the study of the MB adsorption isotherms. The Freundlich, Langmuir, Temkin, and Harkins–Jura isotherm models have been used in the study. Moreover, the diffusion controlling step has been determined by testing the adsorption data using the intraparticle and D-W diffusion models. Finally, the formulation conditions, such as alginate concentration, crosslinker concentration, crosslinking time and temperature, and adsorbent amount, with alginate biopolymer, have been studied. The synergetic effect between the alginate and the nano-polyacrylonitrile (PAN) and HPAN particles has been investigated. The calculated distribution coefficient (K_d) values were found to be 6.0 and 12.25 L $g^{-1}$for PAN and HPAN, indicating that the PAN is a suitable adsorbent while the HPAN is an outstanding adsorbent.

Keywords: Nano-polyacrylonitrile; Precipitation polymerization; Methylene blue adsorption; Modelling; Formulation

1. Introduction

Protection of water resources on the earth planet from mankind pollution is one of the most challenging goals to achieve worldwide. Industrial, agricultural, and domestic wastes are the leading causes of water system pollution. The growing rate of the earth population increased the industrial wastes enormously in the last decades. Among the industrial wastes, dyes are the most spread one. A broad spectrum of industries produced synthetic dyes contaminated waters such as food, tannery, cosmetics, and textiles, which polluted the wastewater due to their toxicity and non-biodegradability [1]. The annual estimation amount of discharged dyes in the water system is over 100,000 metric tons [2,3]. Textile dyes considered as the most threatening source among other dyes [4,5]. The negative impact of releasing colours in the water system ranging from a direct one on the aquatic lives and indirect ones on the humankind live. Methylene blue (MB) is a cationic dye commonly used all over the world as colouring materials [6].

Different approaches have been investigated for dyes removal from wastewater ranging from chemical to physical ones [7,8]. Each method has its drawbacks. Mainly, adsorption suffers from the limitation of the pollutant transfer from the pollutant medium, the thermal destruction needs for high energy while the biological treatment takes a long

* Corresponding author.

[#] Dedication: This publication to dedicate the memory of our wonderful colleague late Dr. I.I. Abdel-Gawad, Professor of organic chemistry, Department of Chemistry, Faculty of Science, Suez University, Suez, Egypt.

time to perform. Indeed, due to the satisfaction of many requirements such as ease, efficiency, and economy, the adsorption technique comes at the front [9–13]. Combination of the adsorption technique with other technology such as photo-degradation increases its benefits compared with other individual contaminants' removal strategies [14–16].

Among different synthetic polymers, polyacrylonitrile (PAN) is one of the most-used synthetic polymers in the dyes and heavy metals ions treatment process. Polyacrylonitrile (PAN) comes first due to its stable chemical structure, which contains anionic groups [17]. Different forms of PAN have been investigated in the removal of dyes and heavy metals ions from wastewater such as nanoparticles [18,19], grafted polymers [20–22], nanofibers [23] and modified ones [24,25].

This work aims to study the kinetic and isotherm of the methylene blue (MB) adsorption by nano-polyacrylonitrile (PAN) and nano-hydroximated polyacrylonitrile (HPAN) particles and the synergetic effect of the formulation with the alginate on its efficiency.

2. Materials and methods

2.1. Materials

Potassium persulfate extra pure (KPS) from (LOBA Chemie, India), Acrylonitrile 99% (AN) from Sigma-Aldrich, Germany, and ethanol absolute, hydroxylamine hydrochloride (H.A) and sodium hydroxide were purchased from Adwic, Egypt. Finally, MB from Sigma-Aldrich, Germany, was used. Sodium alginate (NaALG) with a medium viscosity was supplied from Sigma-Aldrich Company. Calcium chloride ($CaCl_2$) was provided by Riedel-de Hean Company (Germany).

2.2. Preparation of basic dye solution

MB, $C_{16}H_{18}N_3SCl.3H_2O$, stock dye solution was prepared by dissolving 0.01 g of MB in 1,000 mL distilled water. The dye concentration in the supernatant and residual solutions was determined by measuring their absorbance in 1 cm light-path cell at maximum wavelength of 660 nm using spectrophotometer (Jenway 6305, UK).

2.3. Preparation of polyacrylonitrile and hydroximated polyacrylonitrile nanoparticles

The polyacrylonitrile and its modified counterpart, hydroximated polyacrylonitrile, nanoparticles were prepared according to the method mentioned elsewhere [18]. Acrylonitrile was dissolved in 0.4 KPS solution (H_2O:EtOH; 75:25) to have a final 10% monomer solution. Polymerization was conducted at 75°C in the water bath for 6 h to have PAN nanoparticles (51 nm) with ions exchange capacity 0.01 meq/g. The PAN particles were modified with 5% hydroxylamine solution at 70°C for 5 h to have HPAN nanoparticles (208 nm) with ions exchange capacity of 0.15 meq/g. For the same amount of polymers, the surface area of PAN is four times the surface area of HPAN.

2.4. Preparation of PAN-based alginate composite beads

A definite weight of alginate was dissolved in 20 mL hot distilled water to have solution of final concentration ranging between 1% and 5%. Then 0.1–1.0 g of PAN or HPAN was mixed thoroughly to have a homogenous mixture. The mixture was later dropped in calcium chloride solution (1%–5%) at 30°C–60°C and left to harden for 30–120 min. The composite beads were then collected and washed with distilled water to remove the excess of calcium chloride.

2.5. Batch MB adsorption experiments

Definite weight of free PAN or HPAN (0.2 g), or immobilized in 20 mL alginate beads, was mixed with 50 mL of MB dye (10 ppm) at 200 rpm. The adsorption experiments were conducted at room temperature for 180 min.

After the completion of the adsorption cycle, the HPAN particles immobilized with the adsorbed MB were regenerated by washing in 50 mL of HCL (1%) for 1 h at room temperature, washed with water and stir in 50 mL of NaOH (1%) for 1 h; then washed with water for six consecutive times to test the reusability.

The dye removal percentage was calculated according to the following formula:

$$\text{Removal}(\%) = \left[\frac{(C_0 - C)}{C_0}\right] \times 100 \quad (1)$$

where C_0 and C (both in mg/L) are the initial concentration and the concentration at any time, respectively.

The removal capacity was calculated according to the following formula:

$$q(\text{mg/g}) = \frac{V(C_0 - C_t)}{M} \quad (2)$$

where q is the uptake capacity (mg/g); V is the volume of the MB solution (mL), and M is the mass of the PAN or HPAN (g).

2.6. Characterization

2.6.1. FTIR analysis

Analysis by infrared spectroscopy investigating the PAN, HPAN, and MB-HPAN nanoparticles was carried out using Fourier transform infrared spectrophotometer (Shimadzu FTIR-8400 S, Japan).

2.6.2. Thermal gravimetric analysis

Thermal gravimetric analysis (TGA) investing the PAN, HPAN, and MB-HPAN nanoparticles were carried out using a Shimadzu Thermal Analyzer 50 (Japan).

2.6.3. SEM micrographs

SEM micrographs for the PAN, HPAN, and MB-HPAN nanoparticles were carried out using analytical scanning electron microscope (JEOL JSM 6360LA, Japan).

3. Results and discussion

3.1. Effect of Methylene Blue concentration

Variation in the MB concentrations affected the adsorption capacity of the PAN and HPAN nanoparticles, as shown

in Fig. 1. It can be seen that increasing the MB concentration up to 20 ppm increased the adsorption capacity linearly. Further increase of the MB concentration up to 50 ppm led to a lower rate of increment of the adsorption capacity. Such behaviour is an indication of the closeness reach to the saturation of the adsorption centres over the polymer matrices surfaces. The HPAN nanoparticles show higher adsorption capacity than the PAN counterpart. Both adsorbents show the maximum capacity at 50 ppm; 8 ppm and 6.88 ppm for HPAN and PAN. Our results follow the other published results [22,24,25].

3.2. Sorption isotherm models

Sorption isotherms are mathematical models that describe the distribution of the adsorbate species among solid and liquid phases and are thus crucial from the chemical design point of view. The results obtained on the sorption of MB onto the synthesized PAN and HPAN were analyzed by the well-known models given by Freundlich, Langmuir, Temkin, and Harkins–Jura. The sorption data obtained for equilibrium conditions have been analyzed by using the linear forms of these kinds of isotherms.

The Freundlich isotherm is a widely used equilibrium isotherm model but provides no information on the monolayer sorption capacity, in contrast to the Langmuir model [26,27]. The Freundlich isotherm model assumes neither homogeneous site energies nor limited levels of sorption. The Freundlich model is the earliest known empirical equation and is shown to be consistent with the exponential distribution of active centres, characteristic of heterogeneous surfaces [28].

$$\ln q_e = \ln K_F + \frac{1}{n_f}\ln C_e \tag{3}$$

where K_F is the Freundlich constant depicting adsorption capacity, and n_f is a constant indicating adsorption intensity. With plotting $\ln q_e$ against $\ln C_e$, a straight line with slope $1/n_f$ and intercept $\ln K_F$ was obtained. The intercept of the line, K_F, indicates roughly of the adsorption capacity with slope, n, as an indicator for adsorption effectiveness. For the sorption isotherms, initial MB concentration was varied while the pH and temperature of the solution, the agitation speed and sorbent weight in each sample were held constant.

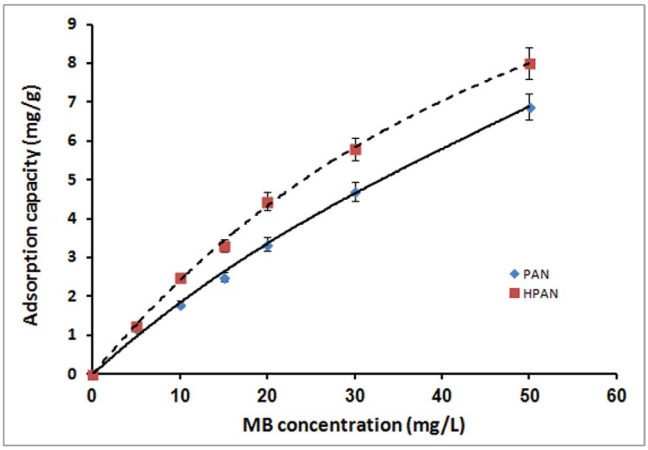

Fig. 1. Effect of the MB concentrations on the adsorption capacity of the PAN and HPAN nanoparticles.

Linear fits of sorption data of the MB were given in Fig. 2a. According to the correlation coefficient (R^2) values, 0.8611 and 0.9191 for PAN and HPAN, it was demonstrated that the removal of MB using HPAN polymer obeyed the Freundlich isotherm better than the PAN polymer. The values of Freundlich constants n_f and K_F that were estimated from the slope and intercept of the linear plot were 2.87 and 1.74 for PAN and 3.69 and 3.42 for HPAN. From the estimated value of n_f, it is found that $n_f > 1$ indicates favourable sorption for MB using both synthesized PAN and HPAN nanoparticles [29]. The adsorption capacity of the HPAN is double than that of the PAN counterpart.

The Langmuir equation, which is valid for monolayer sorption onto a completely homogeneous surface with a finite number of identical sites and with negligible interaction between adsorbed molecules, is given by the following equation [30]:

$$\frac{C_e}{q_e} = \frac{1}{q_m K} + \frac{C_e}{q_m} \tag{4}$$

where q_e is the amount adsorbed (mg/g), C_e is the equilibrium concentration of the adsorbate ions (mg/L). The q_m and K are Langmuir constants related to maximum adsorption capacity (monolayer capacity) (mg/g) and energy of adsorption (L/mg).

Plotting of C_e/q_e vs. C_e indicates a straight line with $1/q_m$ slope and an intercept of $1/q_m K$. Fig. 3 illustrates the linear plot of the Langmuir equation for the MB removal using the synthesized polymers at various initial MB concentrations. The value of correlation coefficient (R^2) was considered as an indicator of the goodness-of-fit of experimental data on the isotherm model. The R^2 values were 0.7887 and 0.9676 for PAN and HPAN polymers indicating a good mathematical fit of the adsorption date using HPAN polymer than PAN polymer.

Langmuir parameters for MB removal, q_m and K, were calculated from the slope and intercept of Fig. 2b and the computed values of q_m equal to 8.76 and 8.34 mg/g for PAN and HPAN. These results indicate that the HPAN polymer has a higher efficiency for MB removal and lower energy of sorption than that of the PAN polymer; 8.55 and 1.53 L/mg for PAN and HPAN.

To predict whether an adsorption system is favourable or unfavourable, dimensionless separation factor was calculated. R_L is defined as [31] follows:

$$R_L = \frac{1}{1 + KC_0} \tag{5}$$

Values of R_L (Table 1) for the MB removal falling between zero and one show favourable adsorption [32] confirming that the adsorption of the MB onto the synthesized polymers under the conditions used in this study was agreeable by Langmuir isotherm.

Temkin isotherm considered the effects of indirect adsorbent/adsorbate interactions on the adsorption process.

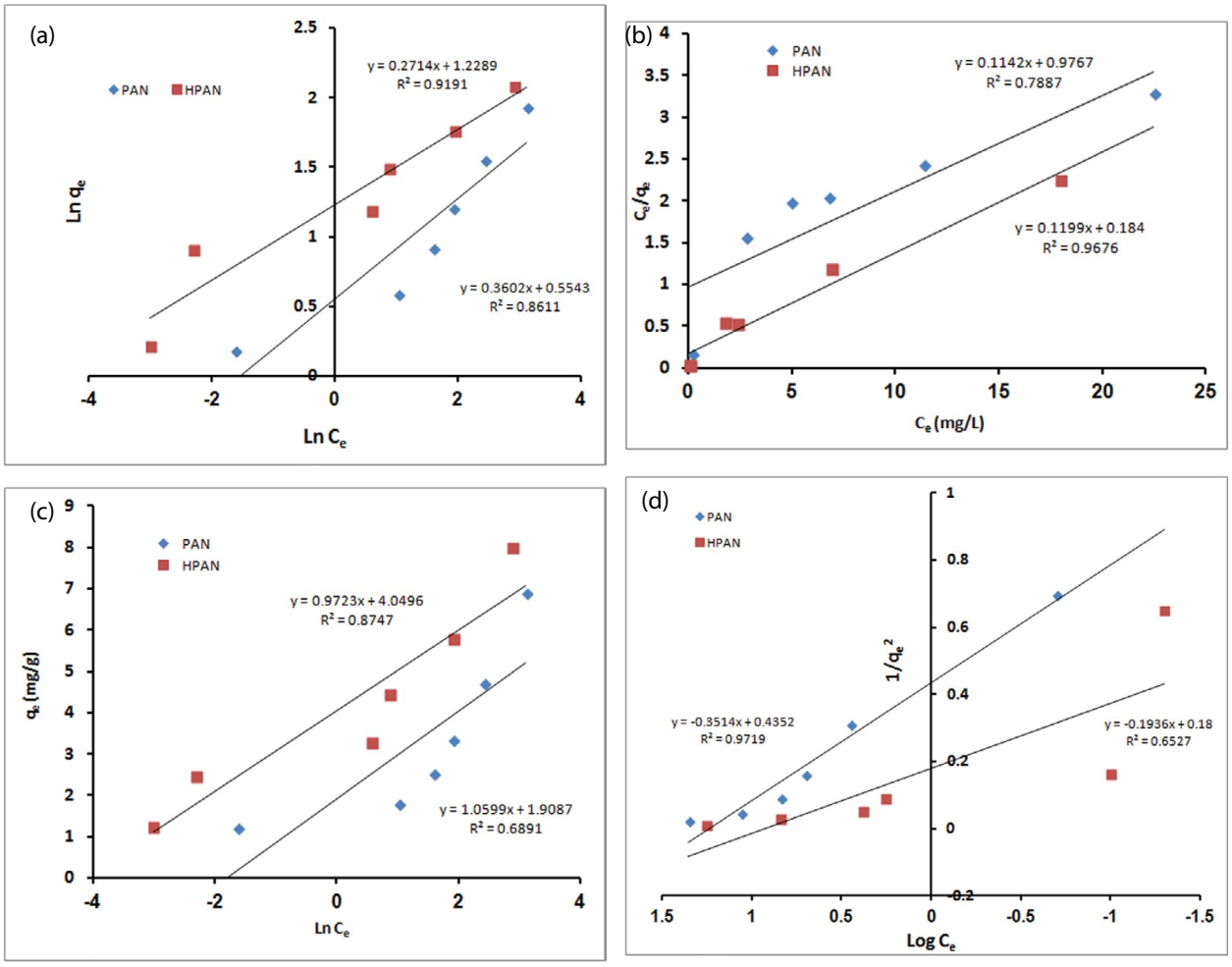

Fig. 2. (a) Freundlich isotherm, (b) Langmuir isotherm, (c) Temkin isotherm, and (d) Harkins–Jura isotherm for the MB removal using the PAN and HPAN nanoparticles with various MB initial solution concentrations.

The heat of adsorption of all the molecules in the layer would decrease linearly with coverage due to adsorbent/adsorbate interactions [33]. It can be expressed in the linear form as [34,35]:

$$q_e = B\ln K_T + B\ln C_e \tag{6}$$

A plot of q_e vs. $\ln C_e$ (Fig. 2c) enables the determination of the isotherm constants B and K_T from the slope and the intercept. From Fig. 4, the calculated K_T is equal to 6.0546 and 64.39 L/g, which represent the equilibrium binding constant corresponding to the maximum binding energy. The constant B that is equal to 1.0599 and 0.9723 J/mol is related to the heat of adsorption for PAN and HPAN, respectively.

Finally, the Harkins–Jura adsorption isotherm can be expressed as [36,37].

$$\frac{1}{q_e^2} = \left(\frac{B_H}{A_H}\right) - \left(\frac{1}{A_H}\right)\log C_e \tag{7}$$

The Harkins–Jura adsorption isotherm accounts to multilayer adsorption and explained by the existence of heterogeneous pores distribution. The value of $1/q_e^2$ plotted against log C_e; where B_H (intercept/slope; mg²/L) and A_H (1/slope; g²/L) are the isotherm constants; Fig. 2d.

The Harkins–Jura isotherm is analogous to the Freundlich model in addition to considering the existence of heterogeneous pore distribution. The model shows the best fit of the results for the PAN polymer where R^2 value equal to (0.9719). The obtained results indicate the formation of multilayers of adsorption and the porous nature of the PAN adsorbent.

All the correlation coefficient, R^2, values and adsorption parameters at equilibrium were obtained from the four equilibrium isotherm models applied for the MB adsorption on the synthesized polymers summarized in Table 2. The Harkins–Jura isotherm model gave the highest R^2 value for PAN (0.9719) showing that this model best described the MB sorption on the synthesized PAN. That suggested the formation of multilayers of adsorption and the porous nature of the PAN adsorbent [36,37]. On the other hand, the Langmuir isotherm model gave the highest R^2 value for HPAN (0.9676) showing that this model best described the MB sorption on the synthesized HPAN. That suggested the monolayer adsorption onto a completely homogeneous surface with a

finite number of identical sites and with negligible interaction between adsorbed molecules [30]. Useful information has been extracted due to the effect of the hydroximation process on the surface nature of the PAN particles and its porosity. The best fitting of the adsorption data of HPAN matrix with the Langmuir isotherm model is the following published work of Abu-Saied et al. [25] used iminated polyacrylonitrile (IPAN) in the removal of MB. Also, Kiani et al. [24] have the same observation using modified PAN with monoethanolamine.

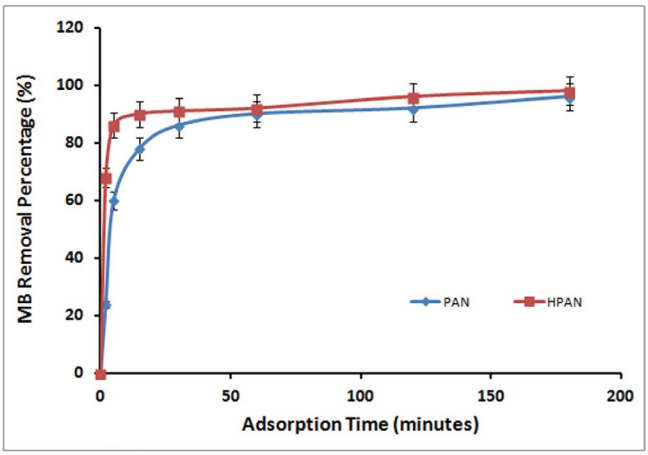

Fig. 3. Effect of the adsorption time on the adsorption capacity of the PAN and HPAN nanoparticles.

3.3. Effect of adsorption time

The impact of varying the adsorption time over 180 min on the removal of the MB dye from 50 mL synthetic solution (10 ppm) using 0.2 g adsorbent at room temperature followed as shown in Fig. 3. From the figure, we can see that almost complete removal of the MB has been reached after 180 min; 96% for PAN and 98% for HPAN particles. However, a clear difference in the rate of removal has been detected in the early stage of the adsorption process.

Table 1
R_L values of PAN and HPAN adsorbents

C_0	R_L (PAN)	R_L (HPAN)
5	0.02286	0.1156
10	0.01156	0.0613
15	0.0077	0.04175
20	0.0058	0.0316
30	0.0039	0.0213
50	0.0023	0.0129

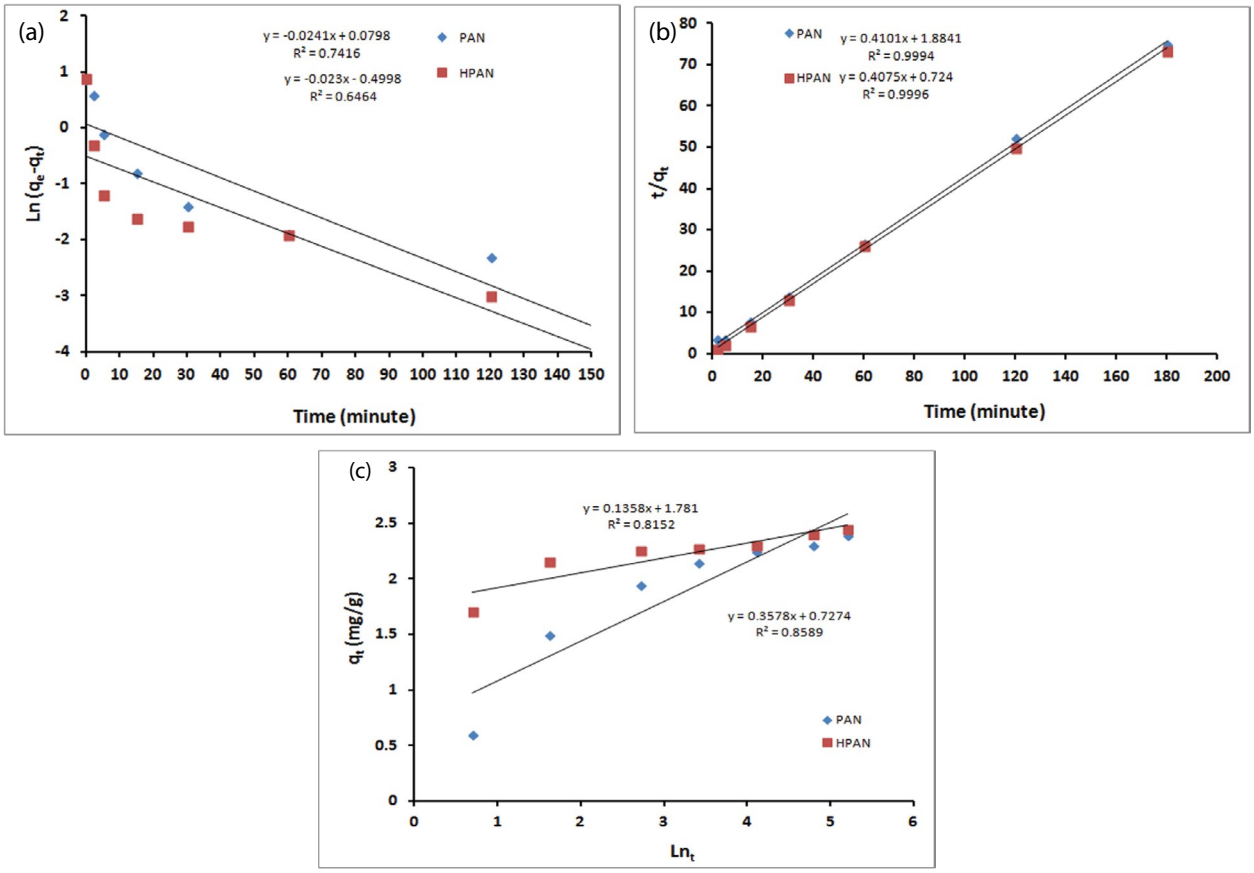

Fig. 4. (a) First order plots, (b) second order plots, and (c) simple Elovich plots for the MB removal using the PAN and HPAN nanoparticles.

Table 2
Parameters and the correlation coefficients of the Langmuir, the Freundlich, the Temkin, and the Harkins–Jura (H-J) isotherm models

Adsorbent	Langmuir isotherm			Freundlich isotherm			Temkin isotherm			Harkins–Jura (H-J)			
	q_{max} (mg/g)	K_L (L mg^{-1})	R^2	K_f (mg/g)	n_f	R^2	B_T (J/mol)	K_T (L/g)	R^2	A_H	V_m (mg/g)	B_H	R^2
PAN	8.7600	8.55	0.7887	1.7400	2.87	0.8611	1.0599	6.0546	0.6891	–2.85	1.5158	–1.24	0.9719
HPAN	8.3400	1.53	0.9676	3.4200	3.69	0.9191	0.9723	64.39	0.8747	–5.16	2.3570	–0.93	0.6527

After 2 min, only 24% removal percentage was obtained using the PAN particles comparing with 68% using the HPAN particles. Such a faster rate of removal is referred to the HPAN particles caused by the additional exchangeable sites resulted from the hydroximation process [18]. Other authors have observed a similar trend used modified PAN with monoethanolamine [24] and iminated PAN [25]. The adsorption capacities of both adsorbents (Table 3) detected at equilibrium are almost equal despite the functionalization of the HPAN with new adsorption sites; 2.4 and 2.45 mg/g for PAN and HPAN nanoparticles. Distribution coefficient, K_d, is a vital parameter to compare the affinity of a pollutant to an adsorbent. It is possible to compare the effectiveness of the adsorbent by comparing the magnitude of the K_d value. Higher the K_d value, the more effective the adsorbent material is. In general, the K_d values of above 1 L/g are considered good, and those above 10 L/g are outstanding [38,39]. It is defined as the mass-weighted partition coefficient between the liquid supernatant phase and the solid phase. The distribution coefficient values of both adsorbents were calculated from dividing the adsorption capacity (mg/g) by the concentration of MB at equilibrium (mg/L). The calculated K_d values were found to be 6.0 and 12.25 L/g for PAN and HPAN, indicating that the PAN is a suitable adsorbent while the HPAN is an outstanding adsorbent.

3.4. Sorption kinetic models

Adsorption is a physiochemical process that involves the mass transfer of a solute (adsorbate) from the liquid phase to the adsorbent surface.

A study of the kinetics of adsorption is desirable as it provides information about the mechanism of adsorption, which is essential for the efficiency of the process.

The most common models used to fit the kinetic sorption experiments are Lagergren's pseudo-first-order model (Eq. (8)) [33], pseudo- second-order model (Eq. (9)) [34], and Elovich model (Eq. (10)) [40].

$$\ln\left(q_e - q_t\right) = \ln q_e - k_1 t \tag{8}$$

$$\frac{t}{q_t} = \frac{1}{k_2 q_e^2} + \frac{t}{q_e} \tag{9}$$

$$q_t = \alpha + \beta \ln t \tag{10}$$

where q_e (mg/g) and q_t (mg/g) are the amount of dye adsorbed at equilibrium and at time t, respectively. k_1 (min^{-1}) and k_2 (g/mg min) are the pseudo-first-order and pseudo-second-order adsorption rate constants, respectively. The Elovich constants are α (mg/g min), the initial sorption rate, and β (g/mg) is the extent of surface coverage and activation energy for chemisorption.

3.4.1. Pseudo-first-order model

The pseudo-first-order kinetic model was the earliest model about the adsorption rate based on the adsorption capacity. The values of the pseudo-first-order constants and

correlation coefficients obtained from the slope of the plot ln ($q_e - q_t$) vs. time in Fig. 4a presented in Table 4. It is indicated that the correlation coefficients are not good enough. Moreover, the estimated values of q_e were calculated from the equation; 1.083 and 0.607 mg/g, have differed from the experimental values, 2.4 and 2.45 mg/g, for PAN and HPAN.

3.4.2. Pseudo-second-order model

The experimental kinetic data were further analyzed using the pseudo-second-order model. By plotting t/q_t against t for MB, a straight line is obtained in all cases. The second-order rate constant, and q_e values were determined from the slope and intercept of the plot in Fig. 4b and presented in Table 4. The values of the correlation coefficients, R^2 for the adsorption of MB on PAN and HPAN were found equal to one. Accordingly, the kinetics of MB adsorption onto PAN and HPAN can be described well by the second-order equation in agreement with other published results [24,25]. That suggests the rate-limiting step in these sorption processes may be chemisorption involving valent forces through the sharing or exchange of electrons between adsorbent and adsorbate [41].

3.4.3. Elovich model

The simple Elovich model is one of the most useful models for describing the kinetics of chemisorption of gas onto solid systems. However, recently, it has also been applied to describe the adsorption process of pollutants from aqueous solutions. Fig. 4c illustrates the plot of q_t against Lnt for the sorption of MB onto PAN and HPAN. From the slope and intercept of the linearization of the simple Elovich equation, the estimated Elovich equation parameters were obtained. The values of β are indicative of the number of sites available for adsorption. The α values are the adsorption quantity when Lnt is equal to zero; that is, the adsorption quantity when t is 1 h is presented in Table 4. This value helps understand the adsorption behaviour of the first step [42]. Also, from this figure it is clear that the Elovich equation does not fit well with the experimental data.

Table 3
Variation of the adsorption capacity (mg/g) with adsorption time

Adsorption time (min)	Q_t (PAN)	Q_t (HPAN)
2	0.6	1.7
5	1.5	2.15
15	1.95	2.25
30	2.15	2.275
60	2.25	2.3
120	2.3	2.4
180	2.4	2.45

3.5. Sorption mechanism models

Following up the adsorption mechanism of any ions onto solid from aqueous phase is going through a multi-step process. Initially, two steps recognized in the liquid phase. The first step is the transport of the ions from the aqueous phase to the surface of the solid particles, which is known as bulk diffusion. This step was followed by diffusion of the ions via the boundary layer to the surface of the solid particles (film diffusion). The last step consequently happens in the solid phase where the ions transport from the solid particles surfaces to its interior pores, known as pore diffusion or intraparticle diffusion. This step is likely to be slow, and therefore, it may be considered as the rate-determining step.

Adsorption of an ion at an active site on the solid phase surface could also occur through chemical reaction such as ion-exchange, complexation and chelation.

The diffusion rate equations inside particulate of Dumwald–Wagner and intraparticle models were used to calculate the diffusion rate of MB on polymer particles. On the other hand, concerning the external mass transfer, Boyd model was examined to determine the actual rate-controlling step for MB removal.

Usually, the sorption process controlled by either the intraparticle (pore diffusion) or the liquid-phase mass transport rates (film diffusion) [43]. Experimenting is a batch system with rapid stirring lefts the possibility that intraparticle diffusion is the rate-determining step [44]. Weber and Morris [45] explored the possibility of affecting the adsorption process via intraparticle diffusion resistance using the intraparticle diffusion model described as follows:

$$q_t = k_{id} t^{1/2} + I \tag{11}$$

where k_{id} is the intraparticle diffusion rate constant. Weber and Morris [45] have figured out the thickness of the boundary layer from values of I. Greater boundary layer effect was noticed with larger intercept [46]. The plot of q_t vs. $t^{0.5}$ is presented in Fig. 5a using PAN and HPAN. Two separate linear portions that represent each line could be observed from the figure. These two linear portions in the intraparticle model suggest that the removal process consists of both surface removal and intraparticle diffusion. While the initial

Table 4
Adsorption parameters of the pseudo-first, the pseudo-second order and the Elovich kinetic models

Adsorbent	Pseudo-first-order				Pseudo-second-order			Elovich		
	$q_{e,exp,}$ (mg/g)	$q_{e,cal,}$ (mg/g)	k_1 (min^{-1})	R^2	$q_{e,cal}$ (mg/g)	k_2 (m^{2}mg^{-1}min^{-1})	R^2	β (g/mg)	α (mg/g min)	R^2
PAN	2.4	1.083	0.0241	0.7416	2.44	1.881	1	0.3578	0.7274	0.8589
HPAN	2.45	0.607	0.4998	0.6464	2.45	0.724	1	0.1358	1.781	0.8152

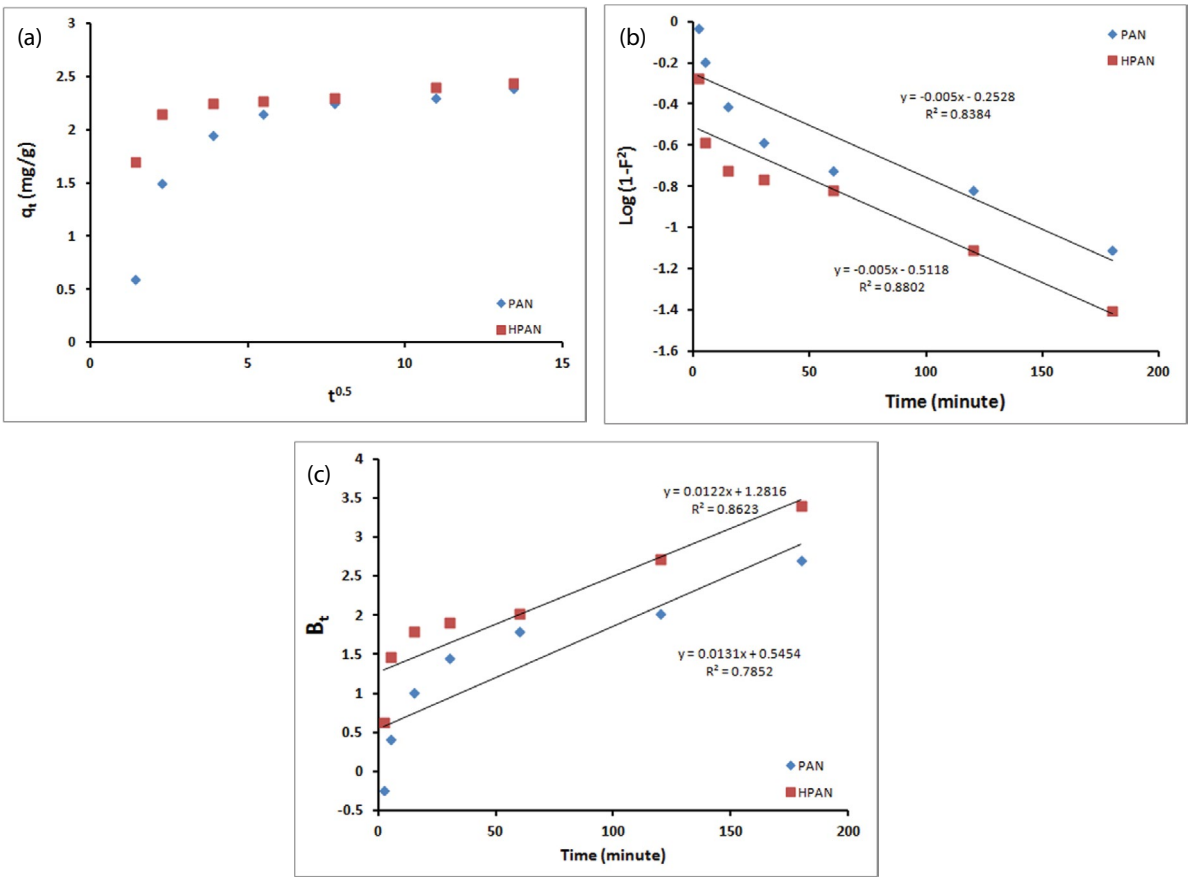

Fig. 5. (a) Intraparticle diffusion plots for the removal of the MB using the PAN and HPAN nanoparticles, (b) Dumwald–Wagner plots for intraparticle diffusion of the MB removal using the PAN and HPAN nanoparticles, (c) Boyd expression for the MB removal using the PAN and HPAN nanoparticles.

linear part of the plot is the indicator of the boundary layer effect, the second linear portion is due to intraparticle diffusion [47]. The intraparticle diffusion rate (K_d), 0.0411 and 0.0217 (mg/g min) for PAN and HPAN, calculated from the slope of the second linear portion and the values of C (1.8693 and 2.155), the intercept, provides an idea about the thickness of the boundary layer. The larger the intercept, the higher is the boundary layer effect [46].

In case of involving the intraparticle diffusion in the sorption process, then a linear relationship would result from the plot of q_t vs. $t^{1/2}$. The intraparticle diffusion would be the controlling step if this line passed through the origin [43]. Fig. 5a confirms that straight lines have not passed through the origin. The difference between the rate of mass transfer in the initial and final steps of the sorption process may cause the deviation of straight lines from the origin. Accordingly, it can be concluded that the pore diffusion is not the sole rate-controlling step [48]. Additional processes, such as the adsorption on the boundary layer, may also be involved in the control of the adsorption rate.

The diffusion rate equation inside particulate of Dumwald–Wagner can be expressed as [49] follows:

$$\log\left(1-F^2\right)=-\left(\frac{K}{2.303}\right)t \tag{12}$$

where K is the diffusion rate constant and the removal percentage, F is calculated by (q_t/q_e). The proper linear plot of log (1–F^2) vs. t (Fig. 5b) indicates the applicability of this kinetic model. The diffusion rate constant K for MB diffusion inside PAN and HPAN particles was found to be –0.011515 min^{-1}.

The kinetic expression further analyzed the adsorption data given by Boyd et al. [50] to characterize what the actual rate-controlling step involved in the MB sorption process.

$$F=1-\left(\frac{6}{\pi^2}\right)\exp\left(-B_t\right) \tag{13}$$

where F is the fraction of solute sorbed at different time t and B_t is a mathematical function of F and given by the following equation:

$$F=\frac{q}{q_\alpha} \tag{14}$$

q and q_α represent the amount sorbed (mg/g) at any time t and at the infinite time (in the present study 30 min). With substituting Eq. (13) into Eq. (14), the kinetic expression becomes:

$$B_t = -0.4978 - \ln\left(1 - \frac{q}{q_\alpha}\right) \quad (15)$$

Thus, the value of B_t can be calculated for each value of F using Eq. (15). The calculated B_t values were plotted against time, as shown in Fig. 5c. The linearity of this plot will provide useful information to distinguish between external transport- and intraparticle-transport controlled rates of sorption. Fig. 5c shows the plot of B_t vs. t, which is a straight line that does not pass through the origin, indicating that film diffusion governs the rate-limiting process [51].

3.6. Adsorbents-alginate composite beads formulation

Separation of nanoparticles from the reaction medium is presenting one of the main challenges retarding commercialization of nanoparticles in the field of adsorbents. Formulation of nanoparticles in composite beads is one of the most obvious solutions to overcome such a problem. Alginate is a biopolymer known by its non-toxicity, biocompatibility and easy of formulations by ionic gelation. In additions, many publications had investigated the removal of different dye from dye effluent solutions and show promising results [52–54]. Formulation of PAN and HPAN nanoparticles with alginate beads will present a solution for the problem of nanoparticles separation and gives the possibility of a continuous application process instead of batch one. Formulation conditions such as alginate concentration, crosslinking time, crosslinking temperature, crosslinker concentration and adsorbent-alginate mass ratio were studied, and the obtained results (within 3%–6% errors) were discussed in the following.

3.6.1. Effect of alginate concentration

The impact of variation of alginate concentration used in the formulation of PAN and/or HPAN on the MB removal percentage was investigated, as shown in Fig. 6a. From the figure, it is clear that the MB removal percentage increases from 39.2% to 57% and from 32.5% to 54% for PAN-alginate composite beads and HPAN-alginate composites, respectively. This trend may be explained based on the increase of the adsorbed sites as a result of increase in alginate concentration. However, the formulation process harms MB removal percentage of PAN and HPAN nanoparticles under the same adsorption conditions; PAN (90%) and HPAN (92%).

Moreover, it is expected that the HPAN-alginate composites beads have a higher MB removal percentage than the PAN-alginate composite beads. However, the obtained results show the reverse where the MB removal percentage of HPAN-alginate composite beads was found lower than that of the PAN-alginate composite beads. The reduction of the MB removal percentage could be explained according to the diffusion barrier presented by the alginate matrix. The consuming of the oxime groups on the HPAN particles surface in binding with calcium ions explains the reduction of the MB adsorption percentage to be less than that of the PAN ones.

3.6.2. Effect of calcium chloride concentration

The impact of variation of calcium chloride concentration on the MB removal percentage investigated, as shown in Fig. 6b. The removal percentage was found to increase from 38% to 48.5% and from 32.5% to 37.77% for PAN and HPAN composites, respectively. The slight increase of the removal percentage could be attributed to the consumption of the surface alginate's carboxylic groups in the ionic gelation process with calcium ions. That leads consequently to reducing the number of the MB adsorbed molecules on the surface of alginate composite beads. Preventing the formation of MB clouds on the surface retards the diffusion of other MB molecules to the interior of the composite beads. As a result, fast diffusion of the MB molecules was obtained and so higher removal percentage.

3.6.3. Effect of the crosslinking time

A slight influence of varying the crosslinking time on the MB removal percentage was observed (Fig. 6c). From the figure, it is clear that the MB removal percentage increases from 41% to 46.2% for the PAN-alginate composite beads and from 35.5% to 42% for HPAN-alginate composite beads with increasing cross-linking time from 30 to 120 min.

3.6.4. Effect of the crosslinking temperature

The result of varying the calcium chloride temperature on the MB removal percentage was investigated in Fig. 6d. From the figure, it was observed that increasing the temperature from 30°C to 70°C has a very slight effect on the MB removal percentage for the PAN-alginate composite beads where risen from 41% to 46.2% and for the HPAN-alginate composite beads from 35.5% to 44%. This behaviour may be referred to as the consumption of the alginate' carboxylic groups on the outer surface of the beads in the crosslinking process with calcium ions. That leads to reducing the amount of adsorbed MB molecules on the surface of the beads and consequently reduces the repulsive effect of the surface MB clouds from preventing the diffusion of the MB molecules from the solution to the interior of the beads.

3.6.5. Effect of the adsorbents content

Fig. 6e shows the impact of varying the HPAN and PAN amount on the MB removal percentage of the HPAN-alginate composite beads and the PAN-alginate composite beads. Two observations have noticed. The first was increased of the MB removal percentage from 40% to 61% for the PAN-alginate composite beads and from 34% to 46.2% for the HPAN-alginate composite beads with the increase of the adsorbent content from 0.1 to 1 g. The second is superior of the MB removal percentage of the PAN-alginate composite beads than the HPAN counterpart. In both cases, the rate of MB removal is shallow compared with the rate of the adsorbent content increase. That is a clear indication of the diffusion barrier formed by the alginate matrix. Increasing the adsorbent content in the alginate composite beads leads to two simultaneous effects. The first is reduction of the alginate matrix porosity and consequently retarded the diffusion of the MB molecules from the bulk solution to the interior

of the adsorbent-alginate composite beads. The second is the formation of high-density clouds of the adsorbed MB molecules on the outer layers of the composites beads, which further reduced the concentration gradient driving force. The accumulation of the two effects leads to the reduction of the adsorption capacities of the composite beads.

3.6.6. Synergic effect of the adsorbent-alginate composite

The synergic effect of formulation of the PAN and HPAN nanoparticles with alginate explored. The MB removal percentage of each of the composite components under the same experimental conditions was evaluated, and the data are presented in Fig. 6f. From the figure, it is evident that bringing two materials having adsorption ability towards MB is not accumulative by necessary. The formulation of the PAN and HPAN nanoparticles solves the problem of separating the adsorbents after completion of the treatment process. indeed the adsorbents lost more than 35% of their capability to adsorb the MB dye especially at higher adsorbent content composite; higher than 0.7 g. At the lower adsorbent content composite, this is not the case. May be this is the area where we can have the advantage of the formulation without losing the native capability of adsorbents to adsorb MB.

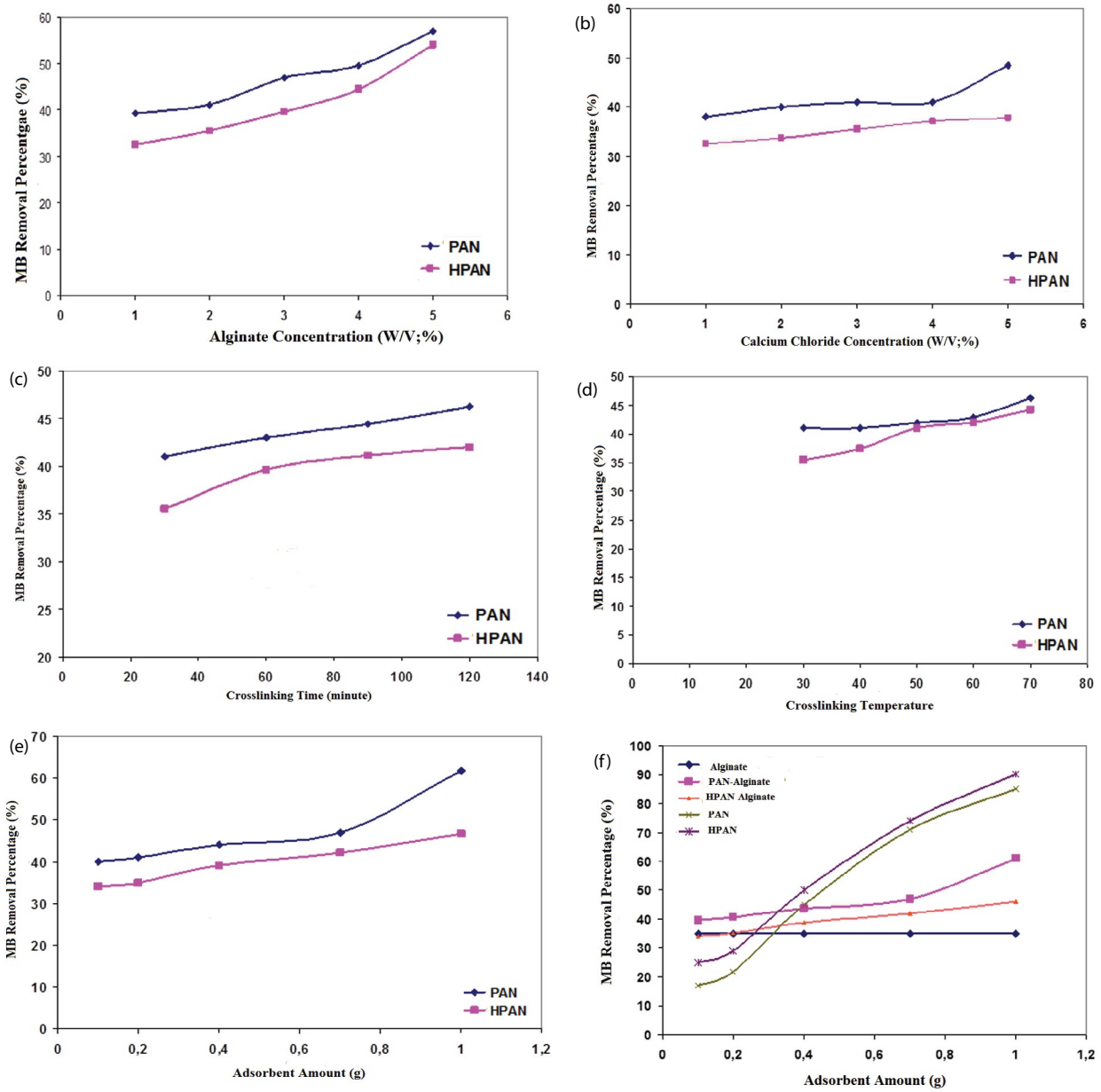

Fig. 6. Effect of (a) alginate concentration, (b) calcium chloride concentration, (c) variation of the cross linking time, (d) variation of the crosslinking temperature, (e) PAN and the HPAN amount on the MB removal percentage of the PAN-alginate composite beads and the HPAN-alginate composite beads. (f) Effect of the adsorbent amount on the MB removal percentage of the alginate beads, PAN, HPAN, PAN-alginate composite beads, and HPAN-alginate composite beads.

Reducing the porosity of the higher adsorbents content' composites beads and increasing the number of the adsorbing sites on the surface of the beads may give explanations. Creating repulsive shield of the adsorbed MB molecules on the beads surface reduces the concentration gradient between the dye solution and the composite beads. That leads consequently to retard the diffusion of the MB from the bulk solution to the interior of the composite beads. Keeping the size of the beads as low as possible along with low adsorbents content may be a solution for having more efficient adsorbents-alginate composite beads for the MB removal.

The following mechanisms for the interaction of adsorbent and dye molecules were proposed:

- Electrostatic interaction between the negative COO^- of the alginate, the negative nitrile groups of the PAN, the negative hydroximic groups of HPAN and the cation groups N^+ of the MB.
- n–π interactions between deprotonated COO^- groups, nitrile groups of the PAN, and hydroximic of the HPAN sorbents as n-donors with the π acceptor sites of the aromatic ring of the MB [55].

3.7. Reusability

The applicability of the HPAN particles was tested for six successive cycles of adsorption and desorption. The data presented in Fig. 7 show that the HPAN particles can adsorb over 90% of MB over six cycles. This result is a promising finding which nominates the HPAN adsorbent for a possible application in the process of wastewater treatment.

3.8. Comparative study

Table 5 presents a comparative study of the MB removal using polyacrylonitrile with chemical modifications. Also, different other adsorbents were included. From the table, it is clear that Salisu et al. [22] removed methylene blue (MB) dye using alginate graft-polyacrylonitrile beads. They found that the Langmuir maximum monolayer coverage of 3.51 mg/g. Kiani et al. [24] developed chelating resins based on polyacrylonitrile (PAN) and monoethanolamine to remove methylene blue from aqueous solution. They found that the maximum adsorption capacity was 52.3 mg/g. Abu-Saied et al. [25] developed iminated polyacrylonitrile (IPAN) and used it as an adsorbent for the removal of Methylene Blue (MB) dye from its aqueous solutions. They found that the Langmuir adsorption capacity (Q_o) 54 mg/g. Natural-based adsorbents such as H. cannabinus-g-PAA and H. cannabinus-g-PAA/PAAM show low adsorption capacity (7.0 mg/g) [56] regardless of grafting with functional polymers. Activated lignin-chitosan blends and brown macroalga show moderately medium adsorption capacity (35–36 mg/g) [57,58]. Inorganic adsorbent such as MOF has moderately high adsorption capacity (326 mg/g) [59]. Our HPAN shows maximum adsorption capacity of 8.34 (mg/g).

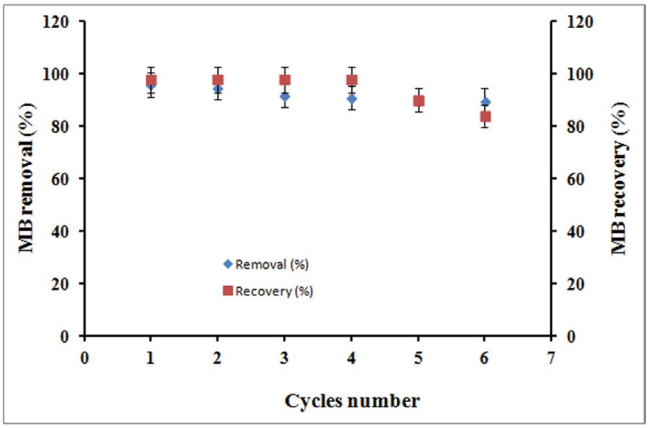

Fig. 7. Effect of the reuse cycle on the MB removal (%) and MB recovery (%).

3.9. Characterization

3.9.1. FTIR analysis

The FTIR spectra of PAN, HPAN, and MB-HPAN were investigated (Fig. 8). The pattern of PAN shows a band at 1,450 cm^{-1} for bending vibration of (–CH_2–) polymeric chain. A characteristic band at 2,245 cm^{-1} attributed to (C≡N) and band at 2,936 cm^{-1} for (C–H) recognized. HPAN pattern shows significant band corresponding to (NH_2) groups at 3,507.7 cm^{-1}, and a band at 1,658 cm^{-1} corresponding to (C=N) bond due to reaction with hydroxyl amine. Also, there is a band at 2,244 cm^{-1} attributed to C≡N with intensity less than PAN, which indicates of incomplete conversion of nitrile groups into oximes ones. At 2,934 cm^{-1}, there is a band corresponding to C–H with less intensity than PAN [13]. MB-HPAN pattern shows overlapping of the MB characteristic bands. A band at 1,600 $cm^{-1}$with band at 1,658 cm^{-1} corresponding to C=N bond due to reaction with hydroxyl amine and resulted in broaden and shifted of the band to 1,637 cm^{-1}, MB characteristic band at 1,334 cm^{-1} with PAN band at 1,360 cm^{-1} and resulted in little broaden of the band. Finally, the MB characteristic band at 890 cm^{-1} overlapped with HPAN band at around 943 cm^{-1} resulted in a stronger and shifted band at 939 cm^{-1} proving the adsorption of the MB onto HPAN particles [60].

3.9.2. Thermal gravimetric analysis

The thermal stability of the PAN, HPAN and MB-HPAN evaluated (Fig. 9). TGA curve of PAN shows the first step

Table 5
Comparison of the MB adsorption capacity of different adsorbents

Adsorbent matrices	Capacity (mg/g)	References
PAN-g-Alginate	3.51	22
PAN-g-monoethanolamine	52.3	24
Iminated polyacrylonitrile (IPAN)	54	25
MOF	326	59
H. cannabinus-g-PAA	7.11	56
H. cannabinus-g-PAA/PAAM	7.00	56
Activated lignin-chitosan Blends	36.25	57–58
HPAN	8.34	This work

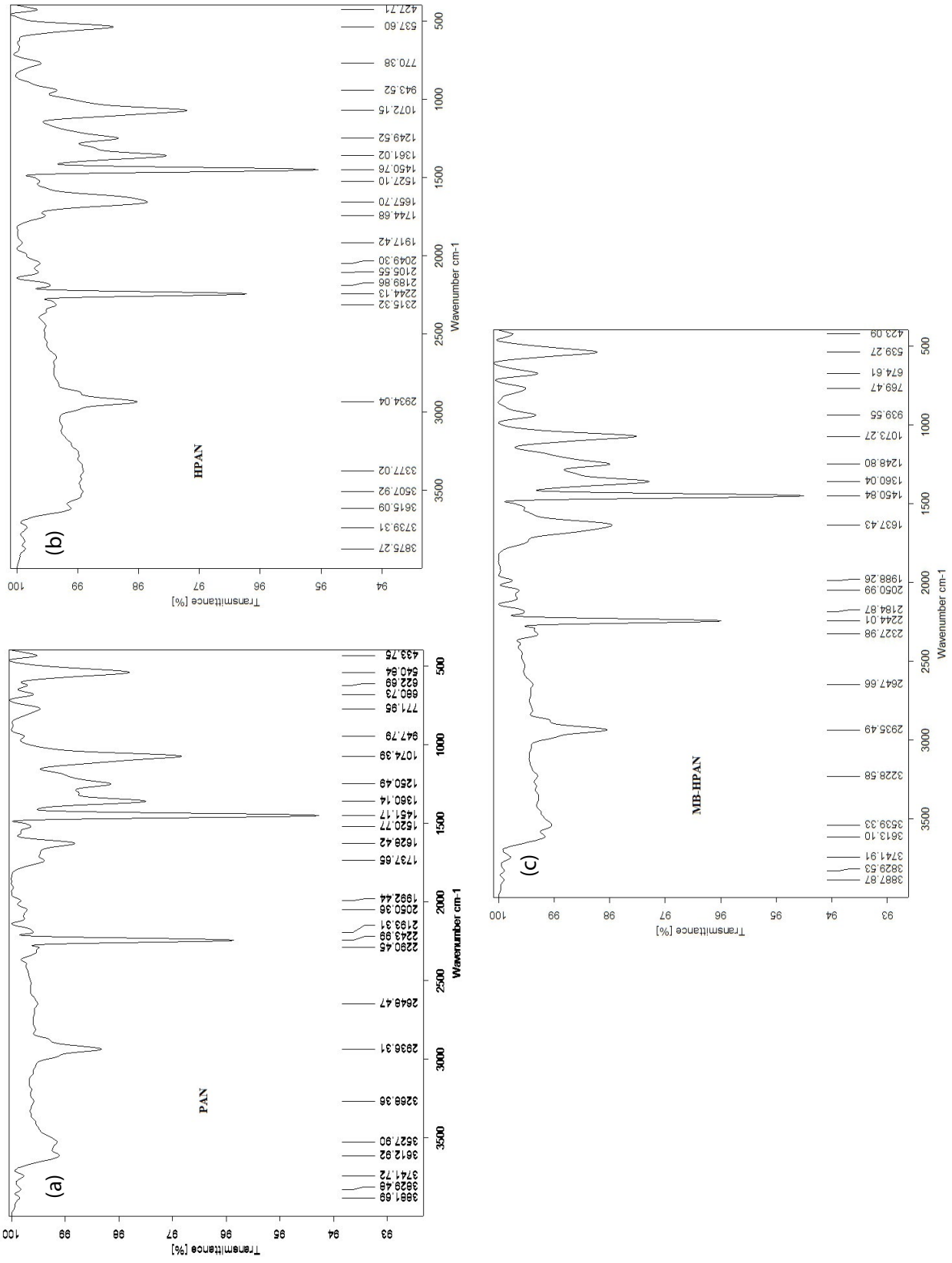

Fig. 8. FTIR analysis of: (a) PAN, (b) HPAN, and (c) MB-HPAN nanoparticles.

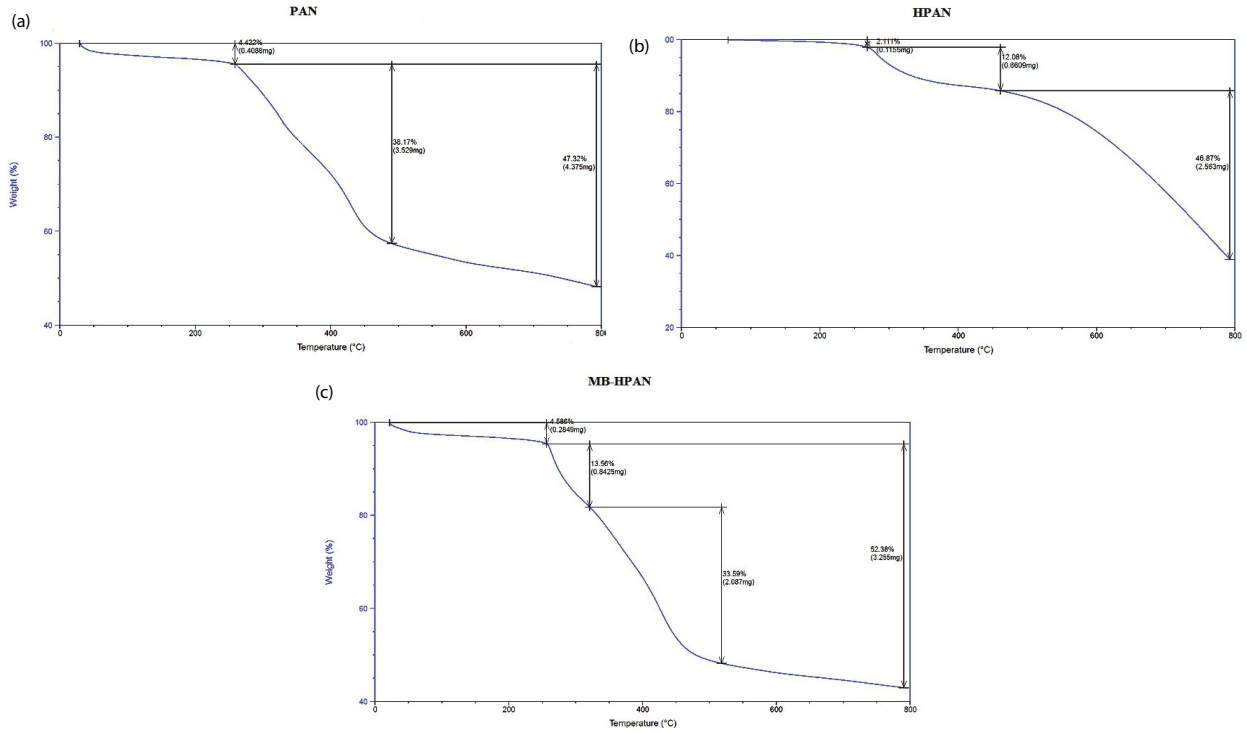

Fig. 9. TGA of: (a) PAN, (b) HPAN, and (c) MB-HPAN nanoparticles.

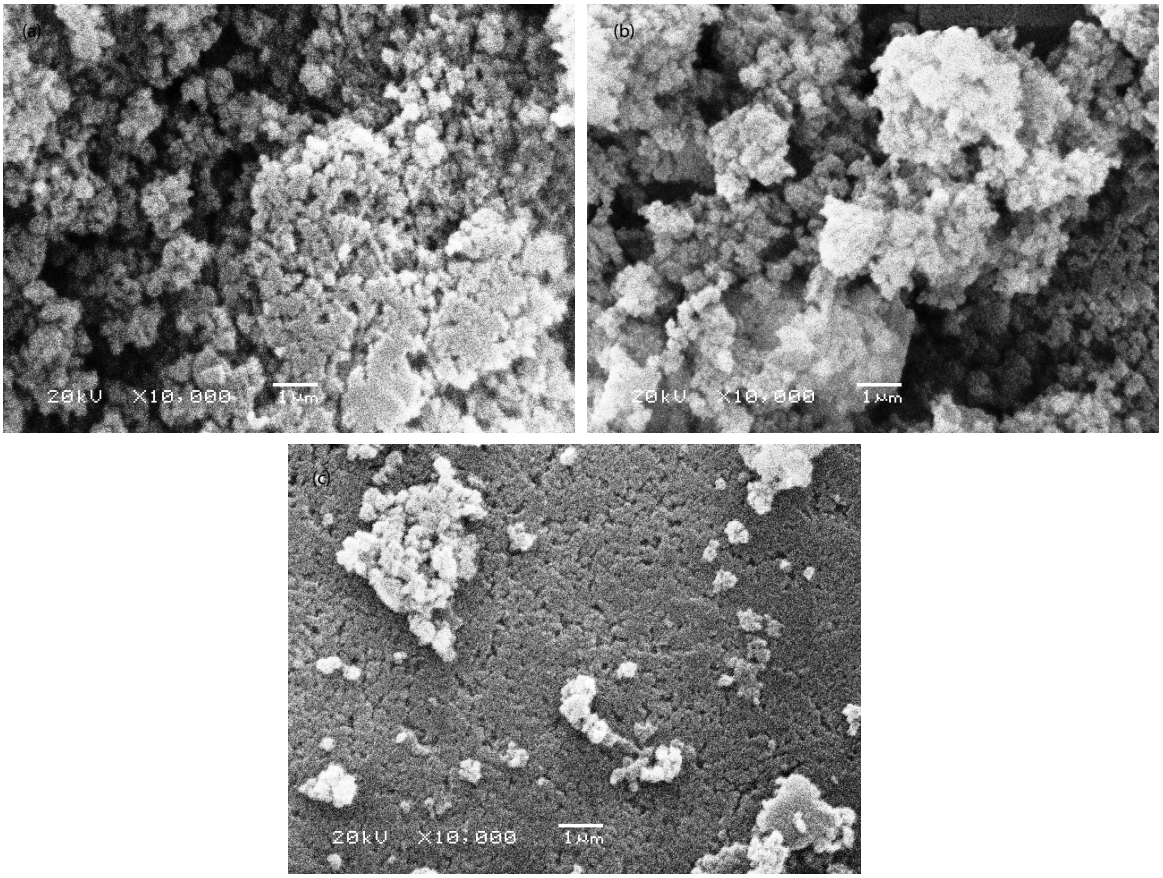

Fig. 10. SEM photographs of: (a) PAN, (b) HPAN, and (c) MB-HPAN nanoparticles.

ended at 260°C, where it lost only 4.4% of its weight. The main stage began at 260°C and end at 490°C with weight loss of 38.17%, and the third step began at 490°C and end at 800°C with weight loss 47%. 32%. The TGA pattern of HPAN contained two main stages. The first main step began at 260°C and ended at 490°C, where it lost around 13.00% of its weight compared with 38.17% of PAN at the same range. The second main step began at 490°C and ended at 800°C with weight loss of around 47.00%. The second main step shows that the HPAN has gain different structure due to the amidoximation process and accordingly acquired thermal stability in this temperature range. The MB-HPAN shows an intermediate TGA pattern between PAN and HPAN, indicating the adsorption of the MB molecules onto HPAN particles. At 800°C, it can be concluded that PAN lost 52% of its weight, HPAN lost 61% of its weight, and MB-HPAN lost 57% of its weight.

3.9.3. Scanning electron micrographs

Examination of morphology structure of PAN, HPAN and MB-HPAN nanoparticles is presented in Fig. 10. From inspection of the figure, it is clear that PAN nanoparticles have an irregular and compact structure. Amidoximation treatment results in kind of changes the structure to be more fused particles but less compact structure as shown in HPAN. The adsorption of MB molecules onto HPAN has an apparent effect. The surface turns to be smoother as a result of the MB molecules coating and filling the pores structure of the HPAN as shown in MB-HPAN.

4. Conclusion

In this study, the kinetic and isothermal studies of the methylene blue (MB) adsorption by nano-polyacrylonitrile (PAN) and nano-hydroximated polyacrylonitrile (HPAN) particles prepared by the precipitation polymerization technique have been performed. The kinetics of the MB adsorption was found to follow the second-pseudo order model. The Harkins–Jura isotherm model gave the highest R^2 value for PAN (0.9719) with maximum adsorption capacity of 1.5158 mg/g. The Langmuir isotherm model gave the highest R^2 value for HPAN (0.9676) with maximum adsorption capacity of 8.34 mg/g suggesting that the formation of multilayers of adsorption and the porous nature of the PAN adsorbent and the monolayer adsorption onto a completely homogeneous HPAN surface with a finite number of identical sites and with negligible interaction between adsorbed molecules.

Moreover, the diffusion controlling step has been determined by testing the adsorption data using the intraparticles, D-W and Boyd diffusion models. According to the obtained results from fitting the data, the film diffusion governs the rate-limiting process. The calculated K_d values were found to be 6.0 and 12.25 L g^{-1} for PAN and HPAN, indicating that the PAN is a suitable adsorbent while the HPAN is an outstanding adsorbent.

Although the formulation of the PAN and HPAN nanoparticles solves the problem of separating the adsorbents after completion of the treatment process, indeed the adsorbents lost more than 35% of their capability to adsorb the MB dye especially at higher adsorbent content composite; higher than 0.7 g. At the lower adsorbent content composite, we can have the advantage of the formulation without losing the native capability of adsorbents to adsorb of the MB.

References

[1] V.K. Gupta, Suhas, Application of low-cost adsorbents for dye removal-a review, J. Environ. Manage., 90 (2009) 2313–2342.

[2] M. Auta, B.H. Hameed, Preparation of waste tea activated carbon using potassium acetate as an activating agent for adsorption of Acid Blue 25 dye, Chem. Eng. J., 171 (2011) 502–509.

[3] M.M. Nassar, M.S. El-Geundi, A.A. Al-Wahbi, Equilibrium modeling and thermodynamic parameters for adsorption of cationic dyes onto Yemen natural clay, Desal. Wat. Treat., 44 (2012) 340–349.

[4] M.M. Ayad, A. Abo El-Nasr, Adsorption of cationic dye (methylene blue) from water using polyaniline nano-tubes base, J. Phys. Chem. C, 114 (2010) 14377–14383.

[5] Y.C. Wong, Y.S. Szeto, W.H. Cheung, G. McKay, Equilibrium studies for acid dye adsorption onto chitosan, Langmuir, 19 (2003) 7888–7894.

[6] A.F. Baybars, Q. Cengiz, K. Mustafa, Cationic dye (methylene blue) removal from aqueous solution by montmorillonite, Bull. Korean Chem. Soc., 33 (2012) 3184–3190.

[7] A.C. Gomes, I.C. Goncalves, M.N. De Pinho, The role of adsorption on nanofiltration of azo dyes, J. Membr. Sci., 255 (2005) 157–165.

[8] P. Sivakumar, P.N. Palanisamy, Adsorption studies of basic red 29 by a nonconventional activated carbon prepared from *Euphorbia antiquorum* L., Int. J. Chem. Technol. Res., 1 (2009) 502–510.

[9] S.P. Dubey, K. Gopal, J.L. Bersillon, Utility of adsorbents in the purification of drinking water: a review of characterization, efficiency and safety evaluation of various adsorbents, J. Environ. Biol., 30 (2009) 327–332.

[10] K. Christian Kemp, H. Seema, M. Saleh, N.H. Le, K. Mahesh, V. Chandraa, K. Kim, Environmental applications using graphene composites: water remediation and gas adsorption, Nanoscale, 5 (2013) 3149–3171.

[11] S. Linjun, X. Guiying, L. Weixi, Y. Huijun, Q. Mingxi, Z. Xian-Man, Q. Chenze, Photodegradation of azo-dyes in aqueous solution by polyacrylonitrile nanofiber mat-supported metalloporphyrins, Polym. Int., 62 (2013) 289–294.

[12] G. Sharma, M. Naushad, A. Kumar, S. Rana, S. Sharma, A. Bhatnagar, F.J. Stadler, A.A. Ghfar, M.R. Khan, Efficient removal of coomassie brilliant blue R-250dye using starch/poly(alginic acid-co-acrylamide) nanohydrogel, Process Saf. Environ. Protect., 109 (2017) 301–310.

[13] S. Ming-Twanga, M.A.A. Zaini, L.M. Salleh, M.A.C. Yunus, M. Naushad, Potassium hydroxide-treated palm kernel shell sorbents for the efficient removal of methyl violet dye, Desal. Wat. Treat., 84 (2017) 262–270.

[14] D. Pathania, D. Gupta, A.H. Al-Muhtaseb, G. Sharma, A. Kumar, M. Naushad, T. Ahamad, S.M. Alshehri, Photocatalytic degradation of highly toxic dyes using chitosan-g-poly(acrylamide)/ZnS in presence of solar irradiation, Photochem. Photobiol., A, 329 (2016) 61–68.

[15] D. Pathania, G. Sharma, A. Kumar, M. Naushad, S. Kalia, A. Sharma, Z.A. ALOthman, Combined sorptional–photocatalytic remediation of dyes by polyaniline Zr(IV) selenotung stophosphate nanocomposite, Toxicol. Environ. Chem., 97 (2015) 526–537.

[16] A. Kumar, G. Sharma, M. Naushad, P. Singh, S. Kalia, Polyacrylamide/Ni0.02Zn0.98O nanocomposite with high solar light photocatalytic activity and efficient adsorption capacity for toxic dye removal, Ind. Eng. Chem. Res., 53 (2014) 15549–15560.

[17] S. Swaminathan, A. Muthumanickkam, N.M. Imayathamizhan, An effective removal of methylene blue dye using polyacrylonitrile yarn waste/graphene oxide nanofibrous composite, Int. J. Environ. Sci. Technol., 12 (2015) 3499–3508.

[18] M.S. Mohy Eldin, S.A. El-Sakka, M.M. El-Masry, I.I. Abdel-Gawad, S.S. Garybe, Removal of methylene blue dye from aqueous medium by nano-polyacrylonitrile particles, Desal. Wat. Treat., 44 (2012) 151–160.
[19] M.S. Mohy Eldin, Y.A. Aggour, M.R. Elaassar, G.E. Beghet, R.R. Atta, Development of nano-crosslinked polyacrylonitrile ions exchanger particles for dyes removal, Desal. Wat. Treat., 57 (2016) 4255–4266.
[20] M.S. Mohy Eldin, M.H. Gouda, M.A. Abu-Saied, Yehia M.S. El-Shazly, H.A. Farag, Development of grafted cotton fabrics ions exchanger for dye removal applications: methylene blue model, Desal. Wat. Treat., 57 (2016) 22049–22060.
[21] M.S. Mohy Eldin,, M.H. Gouda, M.E. Youssef, Yehia M.S. El-Shazly, H.A. Farag, Removal of methylene blue by amidoxime polyacrylonitrile-grafted cotton fabrics: kinetic, equilibrium, and simulation studies, Fibers Polym., 17 (2016) 1884–1897.
[22] A. Salisu, M.M. Sanagia, A. Abu Naim, K.J. Karim, Removal of methylene blue dye from aqueous solution using alginate grafted polyacrylonitrile beads, Der Pharma Chem., 7 (2015) 237–242.
[23] K. Saeed, S.-Y. Park, T.-J. Oh, Preparation of hydrazine-modified polyacrylonitrile nanofibers for the extraction of metal ions from aqueous media, J. Appl. Polym. Sci., 121 (2011) 869–873.
[24] G. Kiani, M. Khodagholizadeh, M. Soltanzadeh, Removal of methylene blue by modified polyacrylonitrile from aqueous solution, CTAIJ, 8 (2013) 121–127.
[25] M.A. Abu-Saied, E.S. Abdel-Halim, Moustafa M.G. Fouda, Salem S. Al-Deyab, Preparation and characterization of iminated polyacrylonitrile for the removal of methylene blue from aqueous solutions, Int. J. Electrochem. Sci., 8 (2013) 5121–5135.
[26] F. Rozada, L.F. Calvo, A.I. Garcia, J. Martin-Villacorta, M. Otero, Dye adsorption by sewage sludge-based activated carbons in batch and fixed-bed systems, Bioresour. Technol., 87 (2003) 221–230.
[27] G. Gode, E. Pehlivan, Adsorption of Cr(III) ions by Turkish brown coals, Fuel Process. Technol., 86 (2005) 875–884.
[28] Y.S. Ho, Effect of pH on lead removal from water using tree fern as the sorbent. Bioresour. Technol., 96 (2005) 1292–1296.
[29] M.M. Dubinin, E.D. Zaverina, L.V. Radushkevich, Sorption and structure of active carbons I. adsorption of organic vapors, Zhurnal Fizicheskoi Khimii, 21 (1947) 1351–1362.
[30] N. Unlü, M. Ersoz, Adsorption characteristics of heavy metal ions onto a low cost biopolymeric sorbent from aqueous solutions, J. Hazard. Mater., 136 (2006) 272–280.
[30] A. Mohammad, A.K.R. Rifaqat, A. Rais, A. Jameel, Adsorption studies on citus reticulate (fruit peel of orange): removal and recovery of Ni (II) from electroplating wastewater, J. Hazard. Mater., 79 (2000) 117–131.
[32] A. Stolz, Basic and applied aspects in the microbial degradation of azo dyes, Appl. Microbiol. Biotechnol., 56 (2001) 69–80.
[33] B.H. Hameeda, L.H. China, S. Rengarajb, Adsorption of 4-chlorophenol onto activated carbon prepared from rattan sawdust, Desalination, 225 (2008) 185–198.
[34] M.I. Temkin, V. Pyzhev, Kinetics of ammonia synthesis on promoted iron catalyst, Acta Physiochim. URSS, 12 (1940) 327–356.
[35] I.A.W. Tan, A.L. Ahmad, B.H. Hameed, Adsorption isotherms, kinetics, thermodynamics and desorption studies of 2,4,6-trichlorophenol on oil palm empty fruit bunch-based activated carbon, J. Hazard. Mater., 164 (2009) 473–482.
[36] K.P.D. Iyer, A.S. Kunju, Extension of Harkins—Jura adsorption isotherm to solute adsorption, Colloids Surf., 63 (1992) 235–240.
[37] A.U. Itodo, H.U. Itodo, Sorption energies estimation using Dubinin-Radushkevich and Temkin adsorption isotherms, Life Sci. J., 7 (2010) 31–39.
[38] W. Yantasee, C.L. Warner, T. Sangvanich, R.S. Addleman, T.G. Carter, R.J. Wiacek, G.E. Fryxell, C. Timchalk, M.G. Warner, Removal of heavy metals from aqueous systems with thiol functionalized superparamagnetic nanoparticles, Environ. Sci. Technol., 41 (2007) 5114–5119.
[39] G.E. Fryxell, Y. Lin, S. Fiskum, J.C. Birnbaum, H. Wu, K. Kemner, S. Kelly, Actinide sequestration using self-assembled monolayers on mesoporous supports, Environ. Sci. Technol., 39 (2005) 1324–1331.
[40] M. Ozacar, I.A. Sengil, A kinetic study of metal complex dye sorption onto pinedust, Process Biochem., 40 (2005) 565–572.
[41] Y.S. Ho, G. McKay, Pseudo-second order model for sorption processes, Process Biochem., 34 (1999) 451–465.
[42] R.L. Tseng, Mesopore control of high surface area NaOH-activated carbon, J. Colloid Interface Sci., 303 (2006) 494–502.
[43] G. Crini, H.N. Peindy, F. Gimbert, C. Robert, Removal of C. I. Basic Green 4 (Malachite Green) from aqueous solutions by adsorption using cyclodextrin-based adsorbent: kinetic and equilibrium studies, Sep. Purif. Technol., 53 (2007) 97–110.
[44] G. McKay, The adsorption of dyestuffs from aqueous solution using activated carbon: analytical solution for batch adsorption based on external mass transfer and pore diffusion, Chem. Eng. J., 27 (1983) 187–195.
[45] W.J. Weber, J.C. Morris, Kinetics of adsorption on carbon from solution, J. Sanit. Eng. Div., 89 (1963) 31–59.
[46] K. Kannan, M.M. Sundaram, Kinetics and mechanism of removal of methylene blue by adsorption on various carbons—a comparative study, Dyes Pigm., 51 (2001) 25–40.
[47] M. Sarkar, P.K. Acharya, B. Bhaskar, Modeling the removal kinetics of some priority organic pollutants in water from diffusion and activation energy parameters, J. Colloid Interface Sci., 266 (2003) 28–32.
[48] V.J.P. Poots, G. McKay, J.J. Healy, Removal of basic dye from effluent using wood as an adsorbent, J. Water Pollut. Cont. Fed., 50 (1978) 926–939.
[49] G. McKay, M.S. Otterburn, J.A. Aja, Fuller's earth and fired clay as adsorbents for dye stuffs, Water Air Soil Pollut., 24 (1985) 307–322.
[50] G.E. Boyd, A.W. Adamson, I.S. Myers, The exchange removal of ions from aqueous solutions by organic zeolites; kinetics, J. Am. Chem. Soc., 69 (1947) 2836–2848.
[51] A.E. Ofomaja, Kinetic study and sorption mechanism of methylene blue and methyl violet onto mansonia (*Mansonia altissima*) wood sawdust, Chem. Eng. J., 143 (2008) 85–95.
[52] L. Boguslavsky, S. Baruch, S. Margel, Synthesis and characterization of polyacrylonitrile nanoparticles by dispersion/emulsion polymerization process, J. Colloid Interface Sci., 289 (2005) 71–85.
[53] T. Biswal, P.K. Sahoo, synthesis of PAN nanoparticles via nonconventional microemulsion technique using Co (II) / EDTA in suit complex, Indian J. Chem. Technol., 14 (2007) 119–125.
[54] J.-M. Lee, S.-J. Kang, S-J. Park, Synthesis of polyacrylonitrile based nanoparticles via aqueous dispersion polymerization. Macromol. Res., 17 (2009) 817–820.
[55] M. Keiluweit, M. Kleber, Molecular-level interactions in soils and sediments: the role of aromatic π-systems, Environ. Sci. Technol., 43 (2009) 3421–3429.
[56] G. Sharma, M. Naushad, D. Pathania, A. Mittal, G.E. El-desoky, Modification of *Hibiscus cannabinus* fiber by graft copolymerization: application for dye removal, Desal. Wat. Treat., 54 (2015) 3114–3121.
[57] A.B. Albadarin, M.N. Collins, M. Naushad, S. Shirazian, G. Walker, C. Mangwandi, Activated lignin–chitosan extruded blends for efficient adsorption of methylene Blue, Chem. Eng. J., 307 (2017) 264–272.
[58] E. Daneshvar, A. Vazirzadeh, A. Niazi, M. Kousha, M. Naushad, A. Bhatnagar, Desorption of Methylene blue dye from brown macroalga: effects of operating parameters, isotherm study and kinetic modeling, J. Cleaner Prod., 152 (2017) 443–453.
[59] A.A. Alqadami, M. Naushad, Z.A. Alothman, T. Ahamad, Adsorptive performance of MOF nanocomposite for methylene blue and malachite green dyes: kinetics, isotherm and mechanism, J. Environ. Manage., 223 (2018) 29–36.
[60] M.A. Olivella, N. Fiol, F. de la Torre, J. Poch, I. Villaescusa, A mechanistic approach to methylene blue sorption on two vegetable wastes: Cork bark and grape stalks, Bioresources, 7 (2012) 3340–3354.